

Electrodynamic response of incoherent metals: Normal phase of iron pnictides

M. S. Laad,¹ L. Craco,^{2,3} S. Leoni,² and H. Rosner²

¹Max-Planck-Institut für Physik Komplexer Systeme, 01187 Dresden, Germany

²Max-Planck-Institut für Chemische Physik fester Stoffe, 01187 Dresden, Germany

³Leibniz-Institut für Festkörper, Werkstofforschung Dresden, 01069 Dresden, Germany

(Received 9 October 2008; revised manuscript received 2 December 2008; published 22 January 2009)

The recent discovery of high-temperature superconductivity in doped iron pnictides is the latest example of unanticipated behavior exhibited by *d*- and *f*-band materials. The symmetry of the superconductor (SC) gap, along with the mechanism of its emergence from the “normal” state, is a central issue in this context. Here, motivated by a host of experimental signatures suggesting strong correlations in the Fe pnictides, we undertake a detailed study of their normal state. Focusing on symmetry-unbroken phases, we use the correlated band-structure method, local density approximation plus dynamical mean-field theory (LDA+DMFT), to study the one-particle responses of both $\text{LaO}_{1-x}\text{FeAsF}_x$ and $\text{SmO}_{1-x}\text{FeAsF}_x$ in detail. Basing ourselves on excellent quantitative agreement between LDA+DMFT and key experiments probing the one-particle responses, we extend our study, undertaking the first detailed study of their normal-state electrodynamic response. In particular, we propose that near-total normal-state incoherence, resulting from strong, *local* correlations in the Fe *d* shell in Fe pnictides, underpins the incoherent normal-state transport found in these materials, and discuss the specific electronic mechanisms leading to such behavior. We also discuss the implications of our work for the multiband nature of the SC by studying the pairing “glue” function, which we find to be an overdamped electronic continuum. Similarities and differences between cuprates and Fe pnictides are also touched upon. Our study supports the view that SC in Fe pnictides arises from a bad-metallic incoherent “normal” state that is proximate to a Mott insulator.

DOI: [10.1103/PhysRevB.79.024515](https://doi.org/10.1103/PhysRevB.79.024515)

PACS number(s): 74.70.-b, 72.10.-d, 74.25.Jb

I. INTRODUCTION

Discovery of high- T_c superconductivity (HTSC) in the Fe-based pnictides¹ is the latest among a host of other ill-understood phenomena characteristic of doped *d*- and *f*-band compounds. HTSC in Fe-pnictides emerges upon doping a bad metal with spin-density-wave (SDW) order at $\mathbf{q}=(\pi,0)$. Preliminary experiments indicate^{2,3} unconventional superconductor (SC). Extant normal-state data indicate a “bad metal” with anomalously high resistivity $O(\text{m}\Omega \text{ cm})$ even at low temperature.¹ These observations in Fe pnictides are reminiscent of *underdoped* cuprate SC. The small carrier density, along with Uemura scaling from muon-spin relaxation (μ -SR) (Ref. 1) similar to hole-doped cuprates, strongly suggests a SC closer to the Bose condensed, rather than a BCS limit. A brief general review⁴ gives a chemist’s overview on the subject.

Several theoretical works have addressed the issue of the “degree of correlated electronic” behavior in Fe pnictides.⁵⁻⁷ This is an important issue, bearing as it does upon a characterization of charge and spin fluctuations: are they itinerant^{8,9} or closer to localized?^{5,6,10} This itinerant-localized *duality* is a recurring theme in correlated systems in general,¹¹ and in fact is at the root of early formulations of the Hubbard model itself.¹²

In Fe pnictides, HTSC results from the Fe *d* band states hybridized with As *p* states: this leads to two hole, and two electronlike pockets¹³ in one-electron band-structure calculations. Within weak-coupling Hartree-Fock random phase approximation (HF-RPA) studies of *effective* two- and four-orbital Hubbard models,^{9,14} this gives a $\mathbf{q}=(\pi,0)$ SDW order, in seeming agreement with inelastic neutron-scattering

(INS) results.¹⁵ Observations of quasilinear (in T) behavior in the resistivity, pseudogap in optical reflectance,¹⁶ and a spin *gap* in NMR (Ref. 3) in *doped* Fe pnictides, among other observations, however, are benchmark features showing the relevance of strong dynamical spin and charge correlations in the pnictides. In analogy with cuprates, this suggests that the Fe pnictides might be closer to a Mott insulator (MI) than generally thought.⁶ Actually, the undoped pnictides of the $A_{1-x}\text{FeAsF}_x$ type with $A=\text{La, Sm}$, the so-called “111” pnictides, show an insulatorlike resistivity *without* magnetic order for $T^* > 137 \text{ K}$,¹ dependent upon the specific Fe pnictide considered. Onset of bad-metallic behavior correlates with a structural [tetragonal-orthorhombic (T - O)] distortion at T^* , *below* which SDW order sets in. This is different from the $A\text{Fe}_2\text{As}_2$ pnictides with $A=\text{Ba, Sr}$ (the so-called “122” pnictides), where the bad-metallic resistivity is observed only above T^* . Nevertheless, as we will discuss below, optical measurements on the 122 family also indicate a non-Fermi Liquid (nFL) metallic behavior at low T . So due care must be exercised when one attempts to classify Fe pnictides into the “weakly” or “strongly” correlated category. The small carrier number seemingly generated upon the structural distortion in the 111 pnictides accords with the observed high resistivity, lending further credence to such a view.

Optical conductivity is a time-tested probe for characterizing the charge dynamics in solids. Specifically, it measures how a particle-hole pair excitation, created by an external photon field, propagates in the system, uncovering the detailed nature of the excitation spectrum itself. In a normal Fermi liquid (FL), low-energy scattering processes leave the identity of an excited electron (hole) intact. This fact, noticed first by Landau, implies a long lifetime for excited *quasiparticles*: near the Fermi surface, their lifetime, $\tau^{-1}(\omega, T)$

$\approx \omega^2, T^2$, greatly exceeds ω, T , their energy. In optical response, this fact manifests itself as the low-energy Drude part (after subtracting the phonon contribution), corresponding to coherent propagation of particle-hole excitations built from such quasiparticles. The Drude parametrization, a lorentzian with half width $\Gamma = \tau^{-1}(\omega, T)$

$$\sigma(\omega) = \frac{ne^2}{m^*} \frac{1}{1 + i\omega\tau(\omega)} \quad (1)$$

describes the low-energy optical response of normal metals. This allows one to estimate the transport relaxation rate and dynamical mass from¹⁷

$$\frac{1}{\tau(\omega)} = \frac{Ne^2}{m_0} \text{Re} \left[\frac{1}{\sigma(\omega)} \right] \quad (2)$$

and

$$m^*(\omega) = \frac{Ne^2}{\omega} \text{Im} \left[\frac{1}{\sigma(\omega)} \right]. \quad (3)$$

With $\sigma(\omega) \approx \Gamma / (\omega^2 + \Gamma^2)$ at low-energy, $m^*(\omega) = m_0$, a constant. As long as the FL survives, even in *f*-band rare-earth metals with *e-e* interactions much larger than the (band) kinetic energy, this observation holds. Observation of a non-Drude optical conductivity in clean metals with low residual resistivity is thus a diagnostic for non-FL charge dynamics, i.e., where $\tau^{-1}(\omega) \approx \omega^2$ and $m^* = \text{const}$ at low energy no longer hold. One can, however, continue to use the Drude parametrization at the cost of having a complicated ω dependence of τ^{-1} and m^* at low energy. Such non-FL optical conductivity in the symmetry-*unbroken* bad-metallic phases is characteristic of several strongly correlated systems, from quasi-one-dimensional Luttinger liquids,¹⁸ high- T_c cuprates up to optimal doping,¹⁹ *f*-electron systems close to quantum phase transitions²⁰ and MnSi,²¹ among others. Additionally, strongly correlated *d*- and *f*-band FL metals routinely exhibit a non-Drude optical response above a low- T scale, the so-called lattice *coherence* scale [$O(1-20)$ K], below which correlated FL behavior obtains.¹¹ So the material diversity and range of distinct ground states exhibited by the above strongly suggests a common underlying origin of the anomalous charge dynamics. The known importance of strong short-ranged electronic correlations in *d*- and *f*-band systems then implies that Mott-Hubbard physics may underlie such generic anomalous features.

On the theoretical side, observation of non-Drude, incoherent, or power-law optical response forces one to discard the Landau FL theory, together with perturbation theory in interactions upon which it is based: an electron (hole), is no longer an elementary excitation of the system. The one-fermion propagator exhibits a *branch cut* analytic structure, leading to power-law fall-off in optics. This reflects the fact that the action of the electronic current operator (within linear-response theory)²² does *not* create well-defined elementary excitations at low energy, leading to an incoherent response.

II. EARLIER WORK

Extant local-density approximation plus dynamical mean-field theory (LDA+DMFT) works on Fe-pnictides give either a strongly renormalized FL (Ref. 5) or an orbital-selective (OS) incoherent pseudogapped metal.⁷ Very good semiquantitative agreement with key features seen in *both* photoemission (PES) and x-ray absorption (XAS) for $\text{SmO}_{1-x}\text{F}_x\text{FeAs}$,^{23,24} as well as with the low-energy (15 meV) kink in PES, is obtained using LDA+DMFT.²⁵ Focusing on the “normal” state of Fe pnictides, is LDA+DMFT adequate for describing their *correlated* electronic structure, or are cluster extensions (cluster DMFT) of DMFT needed? If the observed SDW order has its origin in a Mott-Hubbard, as opposed to a weak-coupling Slater-type SDW picture, one would expect that incorporation of “Mottness”²⁶ is adequate, at least in the symmetry-unbroken phases ($T > T^*$ at $x=0$ and at all $T > T_c$, the SC transition temperature, for doped cases) without SDW and/or SC order. If two-particle spectra, e.g., the optical conductivity, could be described within the *same* picture, this would serve as strong evidence for relevance of large D (DMFT) approaches in this regime. Specifically, given that vertex corrections in the Bethe-Salpeter equations for the conductivity identically vanish in $D = \infty$,²⁷ a proper description of the optical response of $\text{SmO}_{1-x}\text{F}_x\text{FeAs}$ within DMFT would imply negligible vertex corrections, justifying use of DMFT *a posteriori*.

An optical study on La and Sm oxypnictides has already been carried out.^{28,29} While detailed spectral weight analysis remains to be done, characteristic strong correlation features are already visible: a small “Drude” peak, weak midinfrared feature, and a slowly decreasing contribution up to high energy, $O(2.0)$ eV in La pnictides, and a power-law-like decay of the reflectance in Sm pnictide all testify to this fact, and accord with their bad-metallic resistivity. Onset of SC in $\text{SmO}_{1-x}\text{FeAsF}_x$ results in reflectivity changes over a broad energy range,²⁹ a characteristic signature of underlying “Mottness.” Apart from these common features, there are quantitative differences in results from different groups.^{28,29} These can be traced back to the fact that while an effective-medium approximation is invoked for $\text{SmO}_{1-x}\text{FeAsF}_x$,²⁹ no such analysis is performed for $\text{LaO}_{1-x}\text{FeAsF}_x$.²⁸ Given the intrinsic polycrystal nature of the samples used by both, as well as the differences in analysis, this may not be surprising. Optical work on single-crystal samples is thus highly desirable; this may be close at hand. Nevertheless, with these caveats, these observations are strongly reminiscent of cuprates up to optimal doping,¹¹ and constrain theories to understand SC as an instability of an incoherent non-FL metallic state. More recently, Yang *et al.*³⁰ indeed performed a detailed analysis of optics for single crystals of $\text{Ba}_{0.55}\text{K}_{0.45}\text{Fe}_2\text{As}_2$. Slow (in energy, ω) decay in reflectivity and an anomalously large $\tau^{-1}(\omega)$ with sublinear ω dependence, implying no FL quasiparticles, reinforce similar features found in earlier optical results for La and Sm oxypnictides. Further, an extraction of the $\alpha^2 F(\Omega)$ bosonic “glue” (Ref. 30) reveals strong coupling to the low-energy bosonic fluctuation modes (due to interorbital coupled charge-spin density modes). Observation of non-FL quasiparticle features in optics implies that these bosonic modes are themselves

strongly overdamped. Strong inelastic scattering from short-ranged dynamical spin charge and orbital correlations can indeed lead to such behavior, as has been investigated more extensively in the cuprate context. More studies are required to check whether these features are generic for Fe pnictides: in view of incoherent features already seen in all investigated cases, we believe that this will indeed turn out to be the case.

In what follows, we compute the *correlated* band structure and optical conductivity of *both* La and SmO_{1-x}FeAsF_x, extending previous work, where very good semiquantitative agreement with the one-particle spectrum was found.²⁵ We show how “Mottness” in the Fe *d* bands underpins the charge dynamics in Fe pnictides. In particular, we show how an excellent theory versus experiment comparison for the one-particle spectral function (DOS) is obtained for doped LaO_{1-x}FeAsF_x, and build upon this agreement to obtain very good *quantitative* agreement with the *reflectivity* as well. Armed with this agreement, we analyze these theoretical results in detail and predict specific *non-FL* features that should be visible in future experimental work. Finally, we estimate the “glue function,” $\alpha^2F(\omega)$, and propose that it should be understood as an electronic (multiparticle) continuum that can be interpreted as an overdamped bosonic spectrum. We conclude with a brief qualitative discussion of its implications for SC.

III. CORRELATED BAND STRUCTURE

The bare one-electron band structure of both LaOFeAs and SmOFeAs used in this work was computed using the linear muffin-tin orbital (LMTO) scheme³¹ in the atomic sphere approximation (ASA).³² As evidenced in several studies, the overall structures are remarkably similar in both cases, confirming that the active electronic states involve the carriers in the FeAs layers. Shown in Fig. 1, the orbital-induced anisotropies in the band structure are manifest: the *xy* and $3z^2-r^2$ bands are almost gapped at the Fermi energy (E_F), while the *xz*, *yz*, and x^2-y^2 bands have appreciable weight at E_F . The only essential difference between the LDA density of states (DOS) for La and Sm pnictides is that in the latter case, due to larger chemical pressure (caused by the smaller size of Sm relative to La), the LDA band width is slightly [$O(0.5$ eV)] larger. The one-electron part of the Hamiltonian for Fe pnictides is then given by

$$H_0 = \sum_{\mathbf{k}, a, \sigma} (\epsilon_{\mathbf{k}, a} - \epsilon_a) c_{\mathbf{k}, a, \sigma}^\dagger c_{\mathbf{k}, a, \sigma}, \quad (4)$$

where $\epsilon_{\mathbf{k}, a}$ label the five *d* bands and ϵ_a denote the band energies. The interorbital splitting arises from the real crystal field (of S_4 symmetry in Fe pnictides), which lifts the five-fold degeneracy of the atomic *d* shell. This gives the two hole and two electronlike pockets, as apparently observed by de Haas van Alphen (dHvA) studies.³³ To check the accuracy of our LMTO results, we have also carried out the band calculation using the full-potential local-orbital (FPLO) scheme.^{34,35} Comparison between LMTO and FPLO results shows virtually no difference between the two methods, and *small* differences are only visible at high energies. Thus, we use the LMTO DOS as inputs to the multiorbital (MO)

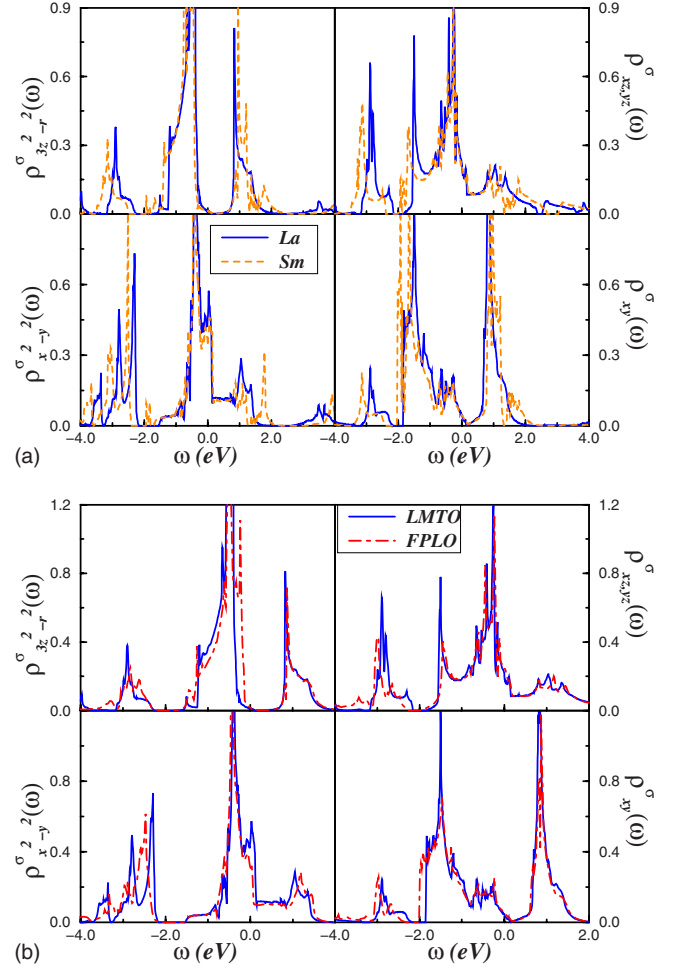


FIG. 1. (Color online) Orbital-resolved LDA density of states (DOS) for the Fe *d* orbitals in LaOFeAs (solid) and SmOFeAs (dashed), computed using the LMTO method. Notice the overall similarity between the two DOSs. This shows that the electronic states generically relevant to Fe pnictides are Fe *d*-band states. The lower panel shows a comparison of the LDA DOS for LaOFeAs computed using both FPLO (dot-dashed line) and LMTO (solid line) methods, showing excellent agreement between them.

DMFT in this work (see also previous work²⁵ for Sm-based Fe pnictides).

However, a direct comparison between LDA results and the PES and/or XAS experiments (which must be considered *together* when a comparison of the theoretical spectral function is attempted) shows substantial mismatch between theory and experiment. Related discrepancies are found in optical studies,²⁸ where the actual plasma frequency, ω_p , is 2–3 times smaller than the LDA prediction. Neither can the high [$O(\text{m}\Omega \text{ cm})$] resistivity be understood within an almost bandlike (free electron) picture. Also, the dHvA study³³ reveals that the LDA bands need to be shifted by 0.2 eV to get a proper fit with experiment. Further, the effective masses are enhanced by a factor of 2–3 over their LDA values (this agrees with the renormalization of the plasma frequency found in optics). Taken together, these features strongly suggest sizable electronic correlations, which, moreover, are also exhibited by a host of other known correlated metals.¹¹

Theoretically, while LDA (LDA+ U) generically accounts for *ground-state* properties of weakly (strongly) correlated systems, their inability to describe excited states (and hence the charge and spin dynamics) in correlated systems is well documented.³⁶ Marrying LDA with DMFT opens the way toward resolving this shortcoming of traditional band structure approaches, and LDA+DMFT has proven successful in describing physical properties of various correlated materials in terms of their *correlated* electronic structures.³⁶

The discussion above clearly shows that incorporation of strong multiorbital electronic correlations is a requirement for a proper description of Fe pnictides. The interaction part is given by

$$H_{\text{int}} = U \sum_{i,a} n_{i a \uparrow} n_{i a \downarrow} + U' \sum_{i,a \neq b, \sigma, \sigma'} n_{i a \sigma} n_{i b \sigma'} - J_H \sum_{i,a,b} \mathbf{S}_{i a} \cdot \mathbf{S}_{i b}, \quad (5)$$

where $n_{a\sigma} = c_{a\sigma}^\dagger c_{a\sigma}$ and \mathbf{S}_a are the fermion number and spin-density operators for an electron in orbital a . We take $U \approx U' + 2J_H$, as is commonly known for transition metal oxides (TMO).³⁶ The relevance of strong correlations in Fe pnictides has been recognized by several authors.^{5,6,10} While these works explicate the important role of MO correlations (in particular, the sensitivity to J_H),⁵ other works⁷ conclude that correlations are weak. This is a highly relevant and open issue in the field of Fe pnictides and their SC: are they weakly correlated itinerant metals, with a conventional BCS-like instability to SC, or are they strongly correlated metals, giving way to SC via a non-BCS-like instability? A detailed comparison with extant experimental results should go a long way toward resolving this important issue.

Here, guided by good success obtained in a theory-experiment comparison of one-particle spectra in our previous study,²⁵ we use LDA+DMFT to compute the detailed optical response in the normal state of La- and Sm-based Fe pnictides. We solve $H = H_0 + H_{\text{int}}$ within MO DMFT. In this study, MO-IPT (MO-iterated-perturbation theory) is employed as the “impurity solver” to solve the impurity model of DMFT. Though not numerically “exact,” it has been shown to be quantitatively accurate for a wide range of correlated d -band materials.^{37,38} If only the FeAs layer states are relevant in Fe-pnictides,¹³ we expect our work to provide a generic picture of charge dynamics in Fe-pnictides. We find excellent quantitative agreement with *both* the one-particle spectral data (PES and/or XAS) as well as two-particle data (reflectance) for the La-based Fe pnictide. Based on this, we argue that Fe pnictides should be viewed as strongly correlated MO systems, with incoherent low-energy behavior and describe the optical response of *both* La- and Sm-based Fe pnictides in detail. Implications of our work for the high- T_c SC in Fe pnictides are touched upon, and intriguing similarities (and differences) with cuprates are highlighted.

Starting with the five Fe d orbitals, we use MO-DMFT to extract the correlated spectral functions for the five d orbitals. We choose values of $U = 4.0$ eV, $J_H = 0.7$ eV, and $U' \approx (U - 2J_H) = 2.6$ eV, as employed in our earlier work.²⁵ These are shown in Fig. 2 for La-based Fe pnictide for three values of electron doping so that $n_{\text{tot}} = \sum_a n_a = (6+x)$, with x

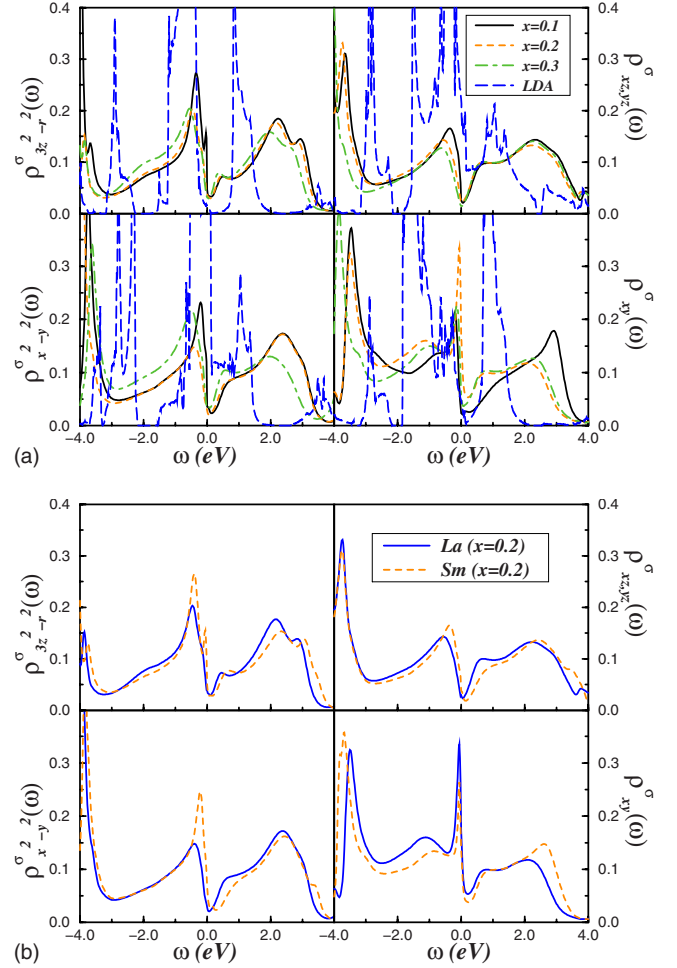


FIG. 2. (Color online) Top panel: Orbital-resolved LDA+DMFT (solid, dashed, and dot-dashed) and LDA (long-dashed) DOS for electron-doped LaOFeAs for three doping values. The parameters are $U = 4.0$ eV, $U' = 2.6$ eV, and $J_H = 0.7$ eV. The drastic modification of the LDA spectra to almost totally incoherent character by large-scale dynamical spectral weight transfer is clearly visible. Bottom panel: Comparison between LDA+DMFT spectra for La- and Sm-based Fe pnictides.

$= 0.1, 0.2, 0.3$, along with the respective LDA DOS. Electronic correlations are seen to lead to dramatic and interesting modifications of the LDA spectra:

(i) The spectra describe an incoherent non-FL metal for *each* of the d bands, with orbital-dependent low-energy pseudogap features. Correspondingly, the imaginary parts of the self-energies (not shown) show deviations from the $-\omega^2$ form at small ω , being consistent instead with a sublinear ω dependence, along with a *finite* value at $E_F (= 0)$, as also seen in our earlier work.²⁵

(ii) In striking contrast to the LDA band structures, the LDA+DMFT band structure shows that multiorbital electronic correlations “self-organize” the spectral functions. While the xy orbital DOS shows the maximum itinerance and has a shape distinct from the others, the much more localized xz , yz , $x^2 - y^2$, and $3z^2 - r^2$ orbital DOSs are seen to closely resemble each other with regard to their line shapes. Dramatic spectral weight transfer (SWT) over large energy

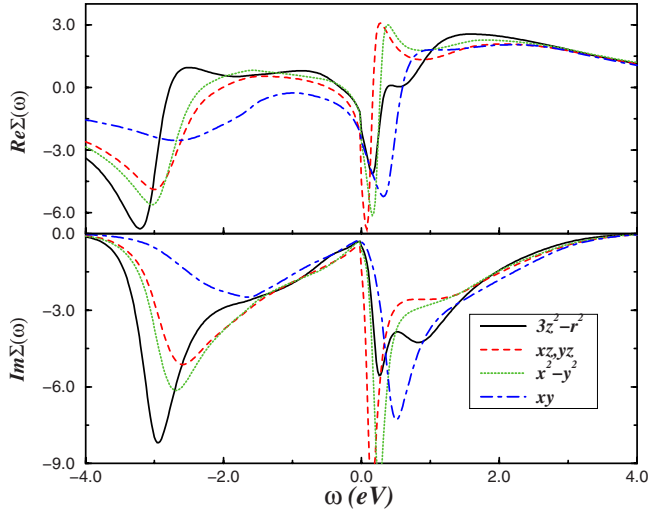


FIG. 3. (Color online) Orbital-resolved LDA+DMFT self-energies for $\text{LaO}_{0.9}\text{FeAsF}_{0.1}$. Upper panel: Real parts, clearly showing the low-energy kink feature, about 21 meV below E_F , in $\text{Re } \Sigma_a(\omega)$ with $a=xz,yz,x^2-y^2,3z^2-r^2$. Lower panel: the corresponding imaginary parts, showing clear sublinear (xz,yz,x^2-y^2) or linear ($xy,3z^2-r^2$) $-\text{in-}\omega$ dependence for $\omega \leq E_F$. These results testify to the incoherent non-FL metallic behavior in doped Fe pnictides in the non-SDW “normal” state).

scales $O(5.0)$ eV is also apparent in the results. In our MO-DMFT calculation, strong incoherent interorbital charge transfer leads to dramatic spectral weight redistribution between the different d -orbital DOS. This is a characteristic also exhibited by other correlated MO systems,³⁹ and points to the relevance of MO correlations in the Fe pnictides.

(iii) There is no OS metallic phase for our choice of parameters, and *all* d -orbital DOS cross E_F . The DMFT results are sensitive to changes in U, U' for fixed J_H , and our results describe a metal very close to the OS metallic one, which occurs for $U \geq 5.0$ eV.⁷

In Fig. 3, we show the orbital-resolved self-energies in the metallic phase of doped $\text{LaO}_{0.9}\text{FeAsF}_{0.1}$. Clear non-FL behavior is evident: *all* self-energies show either a sublinear (xz,yz,x^2-y^2) or linear ($3z^2-r^2,xy$) in ω dependence for $\omega \leq E_F$. Correspondingly, clear kink features are observed in the real parts of $\Sigma_a(\omega)$ for $a=x^2-y^2,3z^2-r^2,xz,yz$. As shown in our earlier work,²⁵ occurrence of these kink features at very low energy is a fingerprint of strong multiorbital correlations in Fe pnictides. Anisimov *et al.*⁴⁰ recently proposed a *weakly* correlated scenario for LaFeAsO , where the DMFT results for $T=1200$ K, using quantum Monte Carlo (QMC) as the impurity solver, are shown. Seemingly, they find that the self-energies show correlated Fermi-liquid behavior ($\approx -\omega^2$) near E_F , even at such high T . There are several problems with such a result: within DMFT, it would imply that Fe pnictides are FL metals even at such elevated T . A perusal of available ARPES and transport data shows that this cannot possibly be the case. As has been discussed by various authors^{5,41} in detail, and as shown by the linear-in- T resistivity immediately above T_c in doped Fe pnictides, the normal state is a non-FL metal, and correlated FL behavior only shows up at much higher hole dopings,

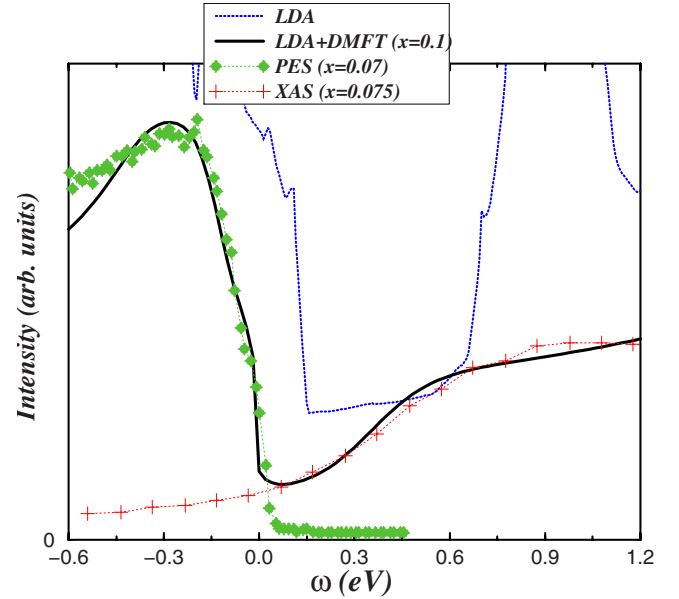


FIG. 4. (Color online) Comparison between the LDA+DMFT result for $\text{LaO}_{0.9}\text{FeAsF}_{0.1}$ (solid line) and angle-integrated photoemission (PES, diamonds) (Ref. 43) and x-ray absorption (XAS, vertical crosses) (Ref. 44) for $\text{LaO}_{0.93}\text{FeAsF}_{0.07}$. As in SmOFeAs (Ref. 25), very good quantitative agreement is clearly seen. In particular, the low-energy kink at -15.0 meV in PES is accurately resolved in the DMFT spectrum. Also notice the substantial improvement obtained by LDA+DMFT over the LDA result (dotted line).

very much like the cuprates.⁴² We emphasize that our finding of sublinear-in- ω behavior of the self-energies at $x=0.1$ is naturally consistent with these observations.

Very similar features have been reported by us for Sm pnictides in an earlier study.²⁵ This is shown in the lower panel of Fig. 2. Given that the LDA bands for Sm-based Fe pnictide are slightly wider than for La-based Fe pnictides, we expect localizationlike features to be more enhanced in La-based Fe pnictides within a Mott-Hubbard picture, as is indeed seen in the comparison. These results imply that strong MO correlations may have a *generic* consequence of self-organizing the correlated spectra, an observation *not* readily seen in the LDA DOS. This may have important consequences, and, for example, could be of aid when one seeks to construct effective *correlation*-based models.

In Fig. 4, we compare our LDA+DMFT results with extant PES and XAS data for $\text{LaO}_{0.93}\text{FeAsF}_{0.07}$.^{43,44} Since only the five d bands have been included in the LDA+DMFT, we restrict ourselves to the energy window (which, however, is rather wide) $-0.6 \leq \omega \leq 1.2$ eV around E_F (this is the region where only the five d bands dominate in the LDA). Clearly, excellent quantitative agreement with *both* PES and XAS results is obtained. In particular, the low-energy pseudogap is faithfully reproduced, as is the detailed form of the line shapes. Taken together with our earlier results on $\text{SmO}_{1-x}\text{FeAsF}_x$,²⁵ this strongly suggests that the FeAs states with sizable d -band electronic correlations are a universal feature of Fe pnictides.

In particular, a noteworthy fact is that for *both* Fe pnic-

tides, a low-energy kink at approximately 15.0–25.0 meV, along with a pseudogap, and strongly asymmetric incoherent features at higher energies (at -0.28 eV in PES and at 0.6 eV in XAS) are clearly resolved.^{43,44} Remarkably, our LDA+DMFT calculation reproduces *all* these features in excellent agreement with both PES and XAS results. The low-energy kink is interpreted as arising from low-energy collective interorbital fluctuations, as discussed earlier²⁵ in detail.

Additionally, two more interesting features are also visible from Fig. 4. First, a good “fit” between the experimental and LDA values of the Fermi energy is achieved by shifting the LDA spectrum *downward* by 0.15 eV. The need for such a shift of LDA DOS in this context has already been noticed earlier⁴³ and attributed to correlation effects. Hitherto, their quantification has not been undertaken. Here, this already arises self-consistently in the MO-DMFT from the MO-Hartree shift mentioned above, bringing the LDA+DMFT value of E_F in very good agreement with experiment. Second, as we will estimate below in optical analysis, the effective plasma frequency is reduced by a factor of 2–3 over its LDA value. This translates into an *average* effective enhancement of the band [local density approximation (LDA)] mass as $(2-3)m_0$, where m_0 is the bare LDA mass. *Both* these observations are completely consistent with the dHvA results, where very similar estimates for the band shift as well as the effective mass were extracted.³³ In addition, the latter is also consistent with the 2–3-fold enhancement in the γ coefficient of the low- T specific heat in $\text{LaO}_{1-x}\text{FePF}_x$.⁴⁵ Taken together, these results constitute a consistent, *quantitative* rationalization of basic one-particle responses in both (La- and Sm-based) pnictides.

IV. OPTICAL CONDUCTIVITY USING LDA+DMFT

We now study the optical conductivity of both doped LaOFeAs and SmOFeAs using the LDA+DMFT propagators for all d orbitals. In $D=\infty$, the computation of the optical conductivity simplifies considerably. This is because the irreducible vertex functions entering the Bethe-Salpeter equation for the evaluation of the current-current correlation function vanish *exactly* in this limit.²⁷ Thus, the optical response is directly evaluated as convolution of the DMFT propagators. For MO systems, the general expression for the real part of the optical conductivity is given by

$$\sigma'_{ab}(\omega) = \frac{2\pi e^2 \hbar}{V} \sum_{\mathbf{k}} \int d\omega' \frac{f(\omega') - f(\omega + \omega')}{\omega} \times \text{Tr}[\mathbf{A}_{\mathbf{k}}(\omega' + \omega) v_{\mathbf{k},a} \mathbf{A}_{\mathbf{k}}(\omega') v_{\mathbf{k},b}], \quad (6)$$

with a, b labeling the various orbitals used in the DMFT calculation. $\mathbf{A}_{\mathbf{k}}(\omega)$ is the one-particle spectral function, a matrix in the orbital sector, and $v_{\mathbf{k},a} = \langle \mathbf{k} | P_a | \mathbf{k} \rangle$ is the fermion velocity in orbital a . The corresponding matrix element of the momentum, P_a , weights the different transitions, and is determined by the band structure. Estimation of the $v_{\mathbf{k},a}$ for Fe pnictides is especially difficult, where, in addition to the d states (which can be written in localized, Wannier-like basis sets), one also has the much more delocalized As p states to contend with. Hence, we simplify our analysis by replacing

this matrix element by a constant, $v_{\mathbf{k},a} = \langle \mathbf{k} | P_a | \mathbf{k} \rangle = v_a$. There are several reasons justifying this approximation:

(i) In an incoherent metal, such as the one we have found for *both* La- and Sm-based Fe pnictides, the short carrier lifetime, $\tau_a = \hbar / \text{Im} \Sigma_a(\omega=0)$, implies that in between successive scattering events, a quasiparticle loses information about its momentum state. Indeed, in such a metal, a quasiparticle in a given \mathbf{k} state has a very short lifetime, during which it decays into incoherent multiparticle states spread out over a large number of single-particle eigenstates (this is the meaning of spectral weight transfer). The band momentum then loses its meaning and can no longer be employed as a good quantum number while computing transition rates.

(ii) Other sources of scattering, neglected in our LDA+DMFT but present in reality, such as phonons and defects, will further degrade the quasiparticle momentum, reinforcing the incoherent aspect due to strong electronic correlations.

In this situation, following Saso *et al.*,⁴⁶ we approximate $v_{\mathbf{k},a}$ by a *single* average carrier velocity for all orbitals. Saso *et al.* and Baldassare *et al.*⁴⁷ showed that this assumption works very well for Kondo insulators FeSi and YbB₁₂ as well as for the classic Mott-Hubbard system V₂O₃, supporting our reasoning above. Moreover, we restrict ourselves to *intra*band transitions.⁴⁸ Both these approximations will turn out to be justified later. With these simplifications, the optical conductivity is written as

$$\sigma'_{ab}(\omega) = \delta_{a,b} v_a^2 \frac{2\pi e^2 \hbar}{V} \sum_{\mathbf{k}} \int d\omega' \frac{f(\omega') - f(\omega + \omega')}{\omega} \times A_{\mathbf{k},a}(\omega' + \omega) A_{\mathbf{k},a}(\omega'), \quad (7)$$

where

$$A_a(\mathbf{k}, \omega) = -\frac{1}{\pi} \text{Im} \left[\frac{1}{\omega - \epsilon_{\mathbf{k},a} - \Sigma_a(\omega)} \right] \quad (8)$$

is the fully renormalized one-particle spectral function for orbital a , and $\Sigma_a(\omega)$ is the corresponding one-particle self-energy. The total reflectivity, $R(\omega) = \sum_a R_a(\omega)$, can be computed using

$$R_a(\omega) = \left| \frac{\sqrt{\epsilon_a(\omega)} - 1}{\sqrt{\epsilon_a(\omega)} + 1} \right|^2, \quad (9)$$

with

$$\epsilon_a(\omega) = 1 + \frac{4\pi i \sigma_a(\omega)}{\omega} \quad (10)$$

being the complex dielectric constant.

Using the Kramers-Krönig (KK) relations, a detailed analysis of the reflectivity, $R(\omega)$, and the optical conductivity can be readily carried out for the normal state. In addition, an extended Drude analysis of the results shines light on the nature of the strong renormalizations caused by MO electronic correlations. In particular, estimation of the frequency-dependent carrier lifetime, $\tau(\omega)$, and effective mass, $m^*(\omega)$, for each orbital state yields microscopic information on the mechanism of incoherent metal formation. Finally, the electronic glue responsible for pairing is estimated there from as¹⁷

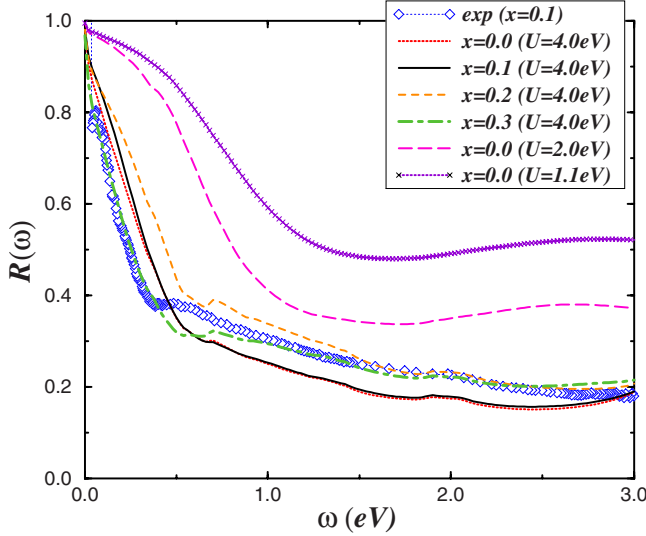


FIG. 5. (Color online) Comparison between the experimental reflectivity for $\text{LaO}_{0.9}\text{FeAsF}_{0.1}$ (Ref. 49) and the LDA+DMFT results for $n_{\text{tot}}=(6+x)$. Very good quantitative agreement over the whole energy range, including the kink in the reflectivity around 0.6 eV is clearly seen for $U=4.0$ eV and $x=0.1$. Also, progressive disagreement between theory and experiment with decreasing U is clear: for $U=1.1, 2.0$ eV, substantial disagreement over the whole energy range is strong evidence for the strongly correlated character of the metallic state in Fe pnictides.

$$\mathcal{F}_a(\omega) \equiv \alpha_a^2 F_a(\omega) = \frac{1}{2\pi} \frac{d^2}{d\omega^2} \left(\frac{\omega}{\tau_a(\omega)} \right) \quad (11)$$

whence microscopic information concerning the detailed structure of the pairing interaction is obtained.

V. RESULTS FOR ELECTRODYNAMIC RESPONSE

We now describe our results. In doing so, we adopt the following strategy:

(i) We use our LDA+DMFT results for doped LaOFeAs , which give a very good description of the one-particle spectral features, Fig. 2, as discussed above. Using the DMFT propagators, we compute the *intra*band optical conductivity of $\text{LaO}_{1-x}\text{FeAsF}_x$. Excellent quantitative agreement with extant reflectivity data as measured²⁸ is obtained, and, building upon this agreement, we describe the optical response (i.e., optical conductivity, plasma frequency, orbital-resolved dynamical masses, and scattering rates) in detail.

(ii) Given the observation that the electronic structure of the Fe pnictides is determined by the electronic states in the FeAs layers, we use our DMFT results for *both* La- and Sm-based Fe pnictides to compute the normal-state electrodynamics in the correlated metal. We provide the *first* theoretical estimates of the anisotropic carrier lifetimes and effective masses as a function of frequency. These results show, in accord with the incoherent metal classification of single-layer Fe pnictides, that their normal state cannot be described within FL theory.

In Fig. 5, we show the theory-experiment comparison for the *reflectivity* of $\text{LaO}_{0.9}\text{FeAsF}_{0.1}$. The experimental result

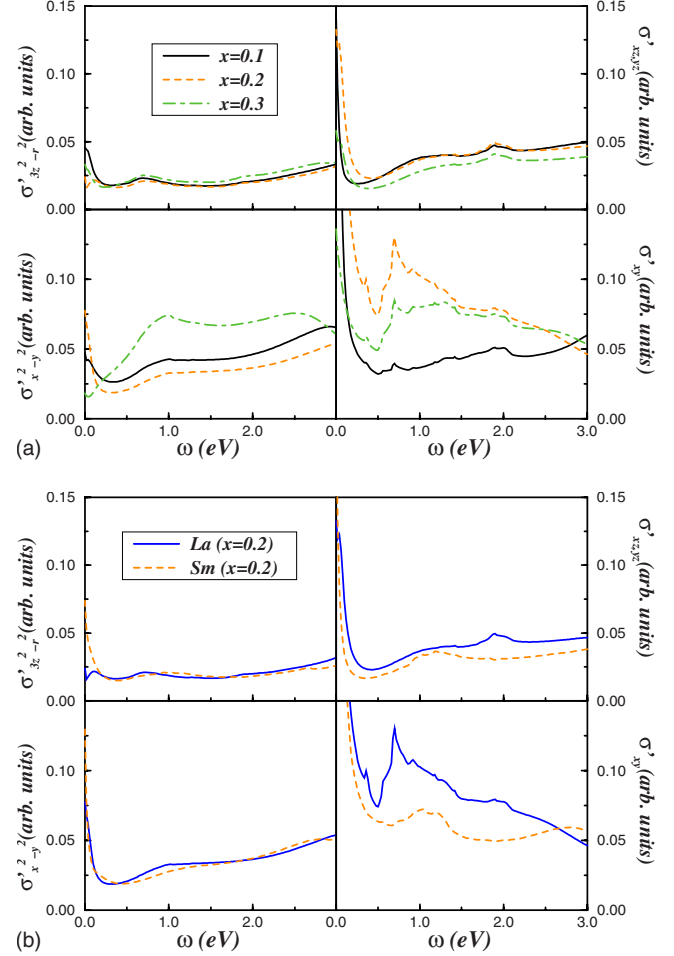


FIG. 6. (Color online) Top panel: Orbital-resolved optical conductivity of $\text{LaO}_{1-x}\text{FeAsF}_x$ for $x=0.1, 0.2, 0.3$, within LDA+DMFT. Apart from the very small quasicohherent component in $\sigma_{xy}(\omega)$, all other orbital components exhibit *incoherent* non-FL responses, with clear wipe-out of the “Drude” response at low energy. Bottom panel: Comparison between the orbital-resolved optical spectra for doped La- and Sm-based Fe pnictides, showing very similar responses in both cases.

was taken from earlier work.²⁸ Quite remarkably, excellent semiquantitative agreement is clearly visible for $U=4.0$ eV, $U'=2.6$ eV, and $J_H=0.7$ eV in LDA+DMFT. To highlight the importance of strong electronic correlations, we have also plotted theoretical results for smaller unrealistic values of $U=2.0$ eV and $U'=1.3$ eV, and $U=1.1$ eV and $U'=0.7$ eV. Clearly, in all respects, the agreement gets worse with decreasing U, U' strongly supporting the strong correlation-based view. This excellent quantitative agreement with *both* one- and two-particle spectra in the normal state of $\text{LaO}_{1-x}\text{FeAsF}_x$ encourages us to make a deeper analysis of transport properties for both La- and $\text{SmO}_{1-x}\text{FeAsF}_x$.

Using Eq. (7), we have computed the optical conductivity, which is shown in Fig. 6 for all d orbitals for both Fe pnictides. Anisotropic responses, dictated both by LDA band structure, as well as by correlation effects (see below), are clearly visible. A very interesting aspect of the results is the observation of strong *incoherent* features in $\sigma_a(\omega)$: a Drude-type peak, with very small weight, exists only in $\sigma_{xy}(\omega)$, and

is even smaller, almost vanishing, in the xz and yz optical response. For all other orbitals, the optical response is totally incoherent, with distinct non-Drude contribution (also see the carrier mass/lifetime results below). Large-scale SWT across huge energy scales $O(4.0)$ eV with doping is also explicit in the results. In the MO-DMFT, this SWT is driven by the *dynamical* correlations associated with large on-site interactions U and U' : the latter causes *interorbital* SWT on the observed scale, and is intimately linked with underlying Mottness in the MO model. The orbital-resolved optical conductivity shows a distinctly non-Drude component, along with a very slow decrease with increasing ω up to high energy, $O(3.0)$ eV. This is observed clearly in Fig. 6 for *both* pnictides. At higher energies, one expects *both* the interorbital transitions, as well as those between the bands neglected within the DMFT to start contributing to $\sigma_a(\omega)$. Thus, one should expect to find good agreement with experiment up to $\omega \approx O(3.0)$ eV. It is rather satisfying to notice that precisely the above features, i.e., non-Drude low-energy part, a slowly decaying (in ω) contribution at higher energies and large-scale SWT with doping have indeed been observed in Fe pnictides. These imply that Fe pnictides should be considered as strongly correlated systems, in the proximity of a MI state.⁶ From the total optical conductivity, $\sigma(\omega) = \sum_a \sigma_a(\omega)$, we have estimated the average plasma frequency from the sum rule

$$\int_0^\infty \sigma(\omega) d\omega = \frac{\omega_p^2}{4\pi}, \quad (12)$$

yielding $\omega_p = 0.76$ eV, in excellent agreement with the experimental estimate of 0.68 eV for $\text{LaO}_{1-x}\text{FeAsF}_x$ with $x = 0.1$. This is a renormalization of a factor of 3 relative to the LDA estimate. For comparison, we have also computed ω_p with reduced U, U' , whence ω_p increases smoothly toward its LDA value (this is also visible from the reflectivity curves, where the kink moves to higher energy with decreasing U, U').

Using the extended Drude parametrization allows us to estimate the frequency-dependent transport scattering rate, $\tau^{-1}(\omega)$, as well as the dynamical mass, $m^*(\omega)$. In Figs. 7 and 8 (top panels), we show these quantities for each orbital, a , as a function of doping. Distinctive non-FL features are clearly evident. We emphasize that these results are valid in the symmetry-unbroken metallic state, i.e., without SDW or SC order: this is the case above T_c in doped Fe pnictides for $x \geq 0.1$. Both τ^{-1} and m^* show distinctly *orbital-selective* non-FL behaviors. With the exception of the xy orbital, $m^*(\omega)$ for the other ($x^2-y^2, xz, yz, 3z^2-r^2$) orbitals continues to increase in a power-law-like fashion or in a fashion consistent with the onset of *incoherent* pseudogap behavior,⁵⁰ down to lowest energy. Correspondingly, the respective scattering rates clearly exhibit a sublinear ω dependence (with anisotropic, $\omega=0$ values) at low energy. Interestingly, the DMFT optical spectra of both La- and Sm-based pnictides show that the dominant low-energy “metallic” contribution comes from the $d_{xz, yz, xy}$ bands, while clear *pseudogap* response is manifest in the $d_{x^2-y^2, 3z^2-r^2}$ channels: the latter are almost Mott localized. This observation is consistent with

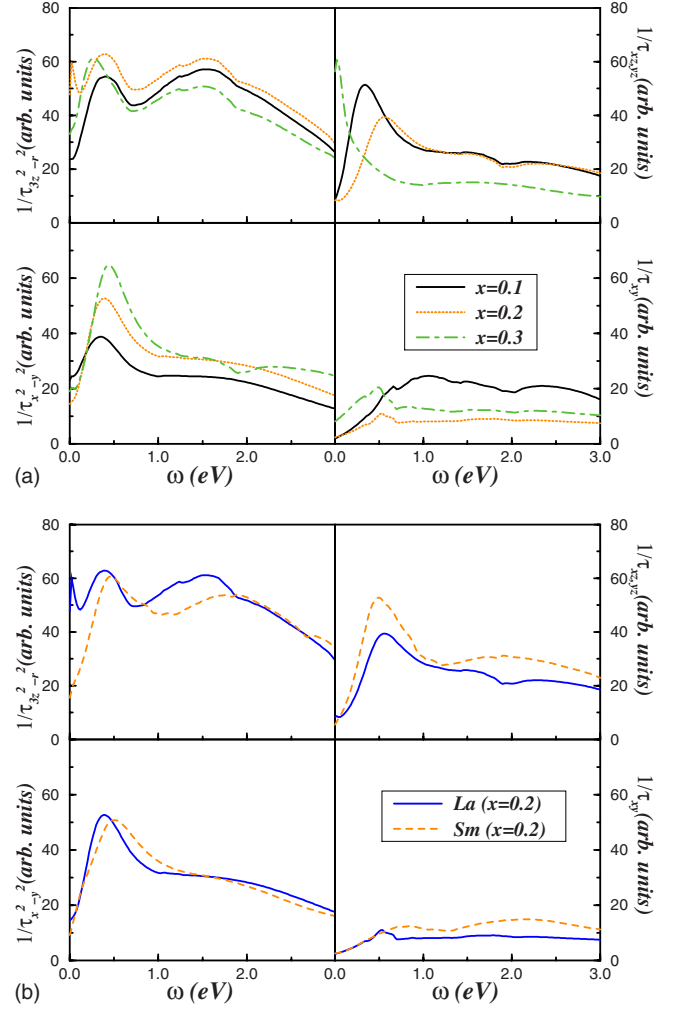


FIG. 7. (Color online) Top panel: Orbital-resolved scattering rates of $\text{LaO}_{1-x}\text{FeAsF}_x$ for $x=0.1, 0.2, 0.3$, within LDA+DMFT. All orbital components exhibit *incoherent* non-FL responses, but the scattering rate for the xy orbital carriers remains most metallic. For the others, the scattering rates exhibit large values at $\omega=0$, in full accord with the emergence of low-energy pseudogaplike features in their corresponding one-particle and optical line shapes. Bottom panel: Comparison between the orbital-resolved scattering rates for doped La- and Sm-based Fe pnictides, showing very similar responses in both cases. Notice the enhanced low-energy incoherence for the La pnictide.

ARPES data,⁵¹ where the *correlated* spectral function is measured; extant results show broadened “quasiparticle” bands on xy , yz , and xz character crossing E_F . In our DMFT, only the “more metallic” xy , yz , and xz bands will then show up as quasicohherent bands crossing E_F , while for the pseudogapped x^2-y^2 and $3z^2-r^2$ bands, the extremely large scattering rates (with a pseudogap) will obliterate these in ARPES.

It is instructive to analyze the differences between the optical spectra for La and Sm pnictides. In the lower panels of Figs. 6–8, we explicitly show these. Clearly, the anisotropic pseudogap features discussed above are more pronounced for the La-based Fe pnictide. To understand this difference, we recall that the LDA band widths for Sm-based

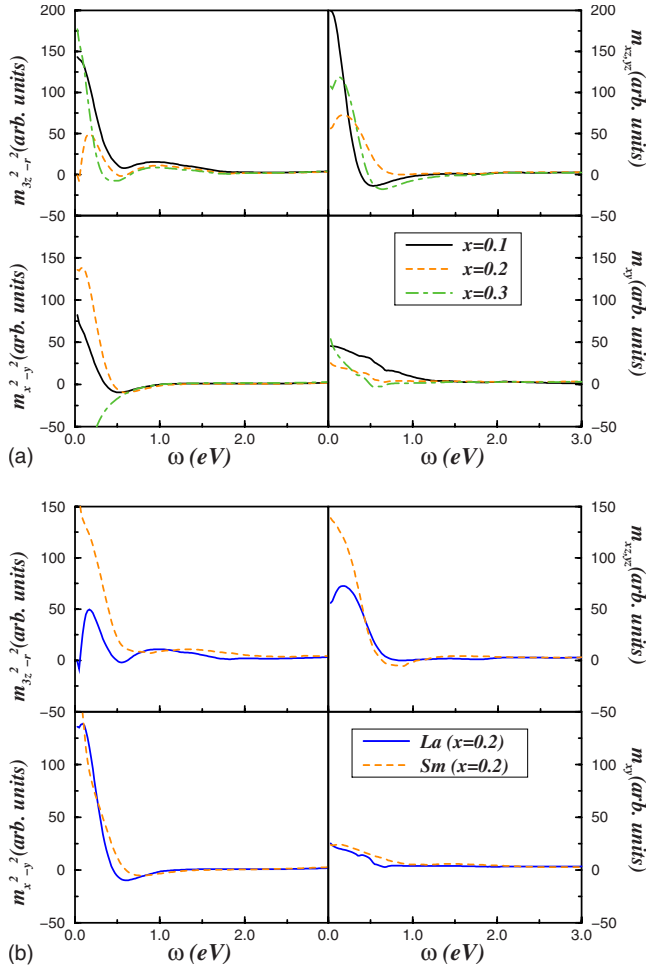


FIG. 8. (Color online) Top panel: Orbital-resolved dynamical masses of $\text{LaO}_{1-x}\text{FeAsF}_x$ for $x=0.1, 0.2, 0.3$, within LDA+DMFT. All orbital components exhibit strong ω dependence at low energy, in line with the incoherent optical responses. Only the mass for the xy orbital carriers seems to approach a constant correlation-enhanced value at low energy. For the others, the dynamical masses exhibit strong ω dependence up to low energy, in full accord with the emergence of low-energy incoherent or pseudogaplike features in their corresponding one-particle and optical line shapes. Bottom panel: Comparison between the orbital-resolved dynamical masses for doped La- and Sm-based Fe pnictides, showing very similar responses in both cases. Notice the enhanced low-energy incoherence for the La pnictide.

Fe pnictide are about $O(0.5)$ eV wider than those for La-based Fe pnictide, an observation that is consistent with the higher chemical pressure induced by the smaller (Sm) ion in the former case. Hence, in our DMFT picture, the correspondingly narrowed d orbitals for La-based Fe pnictide will be closer to Mott localization vis-a-vis those for the Sm-based Fe pnictide; this manifests itself in the observation of pseudogap signatures in $\tau_a^{-1}(\omega)$ and $m_a^*(\omega)$ for La pnictide, while these are weaker for Sm pnictide. Apart from these material dependent differences, the aspect of large normal-state incoherence is clearly reflected in the results for both pnictides.

Finally, we remark that, while such extended Drude analysis for the “single-layer” Fe pnictides remains to be

done with single crystals, a non-FL scattering rate is indeed extracted from the optical spectra for doped BaFe_2As_2 .³⁰ Based on our results, we predict that similar incoherence will characterize the normal-state optical response of the single-layer Fe pnictides as well. The sublinear-in- ω scattering rate is also consistent with the sublinear-in- T dependence of the dc resistivity in doped Fe pnictides⁶ above $T_c(x)$.

VI. DISCUSSION

The lack of any Drude component in the low-energy optical response implies that the symmetry-unbroken metallic state above T_c in the doped Fe pnictides is *not* a FL, in the sense that the one-particle propagators exhibit a branch cut structure, rather than a renormalized pole structure, at low energies.

What is the microscopic origin of the non-FL features found in the DMFT solution? In MO systems, the orbital-resolved hopping matrix elements (diagonalized in the LDA) are very directional, being sensitive functions of orbital *orientation* in the real structure. Further, the d bands are shifted relative to each other because of the action of the crystal field (of S_4 symmetry in Fe-pnictides), and the six d electrons are distributed among all d orbitals. In this situation, strong, MO correlations cause two intimately linked changes:

(i) The static MO-Hartree shift, which depends upon the occupations of each orbital, as well as on the interorbital U' and J_H , renormalizes the on-site energies of each orbital in widely different ways. In particular, it causes interorbital charge transfer between the various d orbitals, self-consistently, modifying their energies and occupations. This effect is also captured in LDA+U approaches. Specifically, the lower-lying orbital(s) in LDA are pushed further down by the MO-Hartree shift, the amount of which is determined by their occupation(s) and by the values of U' and J_H relative to their respective LDA band width(s), and to the *bare* crystal-field splitting in LDA.

(ii) More importantly, the dynamical correlations associated with U , U' , and J_H results in a large-scale transfer of dynamical spectral weight. Small changes in the LDA band structure induced by (i) above (or by changes in external perturbations in general) induce large *changes* in SWT, drastically modifying LDA line shapes.

(iii) Crucially, the renormalized Fermi energy is computed self-consistently in DMFT by requiring consistency with the Friedel-Luttinger theorem; i.e., E_F is computed by demanding that the renormalized Fermi surface encloses the total number of d electrons in the system, as long as no broken-symmetry states are considered.

Generically, as U' increases (J_H is usually fixed for a given d state), the lower-lying subset of d orbitals gets selectively Mott localized; the metallic phase is then the OS metal found recently in various contexts.^{37,52} Once this selective localization occurs within the DMFT, the low-energy physical response is governed by strong scattering between the effectively Mott-localized and the renormalized itinerant components of the matrix spectral function. The problem is thus effectively mapped onto a Falicov-Kimball type of model, as has been noticed in earlier work.^{37,52} Within

DMFT, the itinerant fermion spectral function then shows a low-energy pseudogapped form, while the “localized” spectral function shows a power-law fall off as a function of energy, as long as the renormalized E_F is pinned to the renormalized orbital energy of the localized orbital(s). This is understood from the mapping of the corresponding impurity model to that of the “x-ray edge,”⁵³ where the orthogonality catastrophe destroys FL behavior.⁵⁴ The spectral functions then exhibit asymmetric continua (branch cuts) at low energy, instead of symmetric Abrikosov-Suhl Kondo resonance features, and the metallic phase is *not* a FL. This incoherence is mirrored in the optical responses in $D=\infty$ since the optics is entirely determined by the *full* DMFT one-particle Green’s functions in this limit. This is entirely consistent with our results, and strongly suggests that effects akin to the orthogonality catastrophe, arising from strong incoherent interorbital scattering, produce the incoherent metal behavior in the normal state of Fe pnictides.

This loss of one-particle coherence corresponds to drastic reduction in the carrier kinetic energy, and implies the *irrelevance* of one-particle terms in the RG sense.⁵⁵ Interestingly, this clears the way for two-particle instabilities to take over as T is lowered; they pre-empt the non-FL behavior from persisting down to $T=0$. This could be either:

(i) The $\mathbf{q}=(\pi,0)$ SDW for $x < x_c$. This is in fact further reinforced by the near-nested character of the electron and hole Fermi pockets in the Fe pnictides, already visible in weak-coupling RPA calculations.^{14,56} The SDW instability at $x=0$ is then interpretable as an instability in the particle-hole channel, aided by near FS nesting. That AF-SDW survives the lack of such nesting features away from $x=0$ is an observation which favors a strong-coupling scenario. An intermediate-to-strong coupling version of a similar instability to exactly the same state results from the LDA+DMFT work of Haule *et al.*⁵ A strong-coupling method as used here will yield the same AF instability, in analogy with one-band Hubbard model studies, where the AF ordered state at half filling remains the Néel ordered state, evolving from the Slater type to the Mott-Hubbard type as U/t is increased. Though weak-coupling RPA approaches, valid for small U/t , can indeed give the correct magnetic *ground* states for $U \ll W(=2zt)$, the normal-state incoherence characteristic of Fe pnictides, which are now identified to be in the intermediate coupling limit ($U \approx W$), is beyond their scope. This is because the incoherent part of $G_a(\mathbf{k}, \omega)$ is completely neglected there, and one deals with propagators having only a coherent QP pole structure at low energy. This is valid for small U , but not for $U > W$, the noninteracting bandwidth.

(ii) An unconventional SC for $x > x_c$. This corresponds to an instability in the particle-particle channel. Independent of the precise order-parameter symmetry, a matter of intense debate,^{3,6,8,9} the observation of small superfluid density, short-coherence length, large $2\Delta/kT_c$ ratios, along with large energy scale changes in optical response across T_c , are all hallmarks of a SC closer to the Bose condensation limit, rather than the weak-coupling BCS limit.

Our findings are in accord with Si *et al.*⁶ and Haule *et al.*,⁵ who, along with Baskaran,¹⁰ were the first to recognize the strong-coupling aspect of Fe pnictides. On the other hand, several works address both AF and SC within weak-coupling

scenarios.^{14,56} In the latter, the normal state above T_c is a FL metal, and SC arises via a BCS-like instability of this MO (multiband) FL. In the strong correlation limit, however, the normal state is itself incoherent and so there are no FL-like QPs to pair up into usual BCS-like cooper pairs. In other words, SC must then arise as an instability of an unusual metallic state without FL QPs, or, to rephrase it, directly from overdamped collective multiparticle modes. The *frequency* dependence of the self-energy is important in the latter case, and consideration of the instability of such an incoherent state to the SC state leads to a strongly frequency-dependent SC gap function. In such a “strong-coupling” picture, the physical response functions *in* the SC state are controlled by both the symmetry of the SC order parameter, as well as the strong ω - and T -dependent damping originating in the incoherent normal state. Observation of features such as the absence of the Hebel-Slichter peak in the NMR $T_1^{-1}(T)$ (Ref. 3) and the large-scale modification of the optical spectral weight across T_c (Ref. 29) in the Fe pnictides are strongly suggestive of such a strong-coupling scenario. These features are again reminiscent of cuprates,^{19,57} where the role of normal state (non-FL) incoherence is well documented. To make their role in the Fe pnictides more explicit, we use our optical results to show the pairing glue function for Fe pnictides in Fig. 9. In line with the conclusions extracted from the analysis of the incoherent optical conductivity above, $\mathcal{F}(\Omega)$ shows interesting features. We find the following:

(i) A two “peak” structure, with both peaks strongly broadened by incoherent scattering. We emphasize that this broad two-peak structure arises from the incoherent one-particle propagators, and represents a multiparticle electronic continuum. This could be interpreted as overdamped “bosonic” modes, if one associates the short-ranged strongly coupled spin-orbital modes with the incoherent short-distance components of the conventional bosonic modes used in the itinerant descriptions. It is interesting to notice that similar features, namely, strong non-FL signatures in optics, as well as a strongly damped two-peaked low-energy continuum is also characteristic of high- T_c cuprates up to optimal doping.^{19,57} Thus, our results show that SC arises from an incoherent normal state, and that coupling carriers to an incoherent electronic continuum pairs them up in the SC. Hence, we propose that the underlying Mott-Hubbard physics known to underpin the anomalous responses in cuprates is also at work in the Fe pnictides.

(ii) *All* d -orbital components show up in $\mathcal{F}_a(\omega)$, albeit anisotropically. This supports a MO (multiband) origin for SC pairing in Fe pnictides. Several interesting features are visible upon close scrutiny: the glue function is larger for those (orbitals) bands which are closer to Mott localization, as seen by comparing the respective curves in $\mathcal{F}_a(\Omega)$ and $\rho_a(\omega)$, while the most “itinerant” xy band has the smallest contribution to \mathcal{F} . In other words, there is pronounced orbital-induced anisotropy in the pairing glue function. This should imply an orbital-dependent multiple-gap SC, which may not be inconsistent with recent theoretical indications.^{13,56} In other words, suppression of one-particle coherence [in the DMFT propagators, $G_a(\mathbf{k}, \omega)$] makes two-particle (collective) processes more relevant by enhancing

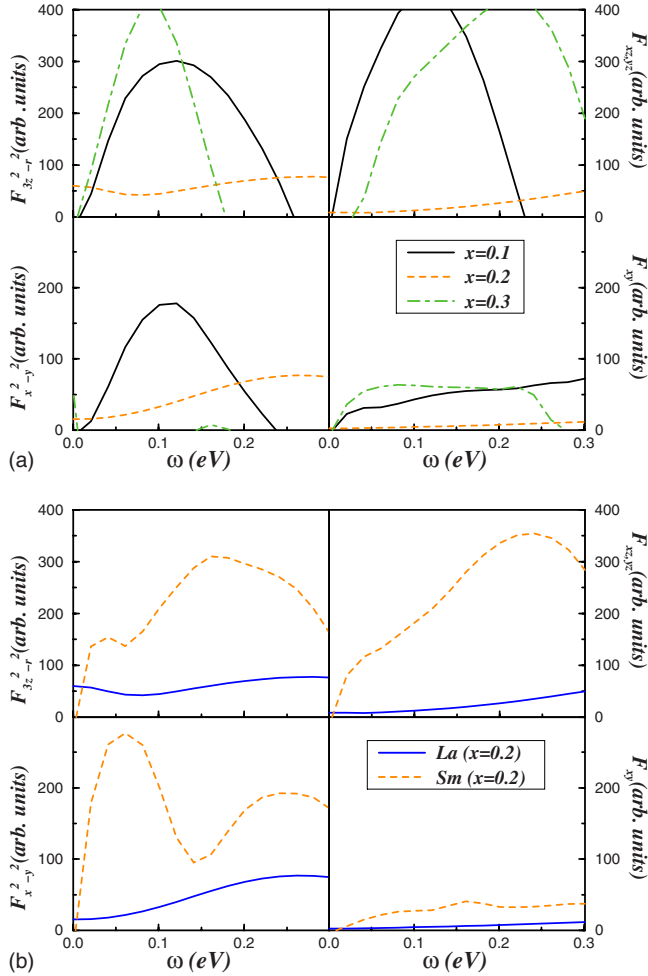


FIG. 9. (Color online) Top panel: Orbital-resolved “glue” functions for $\text{LaO}_{1-x}\text{FeAsF}_x$ for $x=0.1, 0.2, 0.3$, within LDA+DMFT. All orbital components contribute, albeit anisotropically, at low energy. This suggests that the instability to superconductivity in Fe pnictides will involve multiple bands. The lack of any sharp feature shows that the glue is an overdamped electronic continuum (see text). The two-peak structure at low energy is reminiscent of what is seen in high- T_c cuprates and has a multiorbital character. Bottom panel: Comparison between the glue functions for doped La- and Sm-based Fe pnictides, showing similar incoherent electronic continuum features in both cases.

the respective collective susceptibilities in the charge and spin channels. In the doped case, lack of nesting features in the electronlike and holelike Fermi sheets suppresses the $\mathbf{q}=(\pi, 0)$ SDW found for $x=0$, leaving multiband SC as the only relevant two-particle instability. In such a MO-SC, opening up of an orbital-dependent gap should be linked to orbital-dependent coupling of the carriers to the electronic glue via $\mathcal{F}_a(\omega)$: remarkably, a very recent indeed shows exactly this feature.⁵⁸ This agrees qualitatively with our expectations from a strongly orbital-dependent glue function, as derived above. It is also interesting to note that a recent ARPES study on $(\text{Sr}/\text{Ba})_{1-x}\text{K}_x\text{Fe}_2\text{As}_2$ (Ref. 59) also finds quasiparticle kinks in the quasiparticle dispersion in the binding-energy range from 15 to 50 meV, again reminiscent of what is observed in high- T_c cuprates,⁶⁰ but also in three-

dimensional correlated systems like SrVO_3 .⁶¹ The latter fact points to its connection to underlying Mottness characteristic of a correlated system. In our DMFT, we recall that the orbital-resolved DOS show low-energy kinks precisely in the 15–50 meV range (see Fig. 2). These are attributed to low-energy collective interorbital fluctuations,²⁵ and we have shown that the resulting LDA+DMFT DOS gives excellent quantitative agreement with the normal-state kinklike feature in angle-integrated PES.²³ Based on our calculation, we propose that an ARPES measurement done for $(\text{La}/\text{Sm})\text{O}_{1-x}\text{FeAsF}_x$ should uncover kink structure(s) in a similar low-energy (20 meV) range.

Whether additional density-wave instabilities may also interfere with SC is an interesting issue. Two-band model studies^{56,62} do suggest additional channels involving nematic or current instabilities: whether they can seriously compete with SC or remain subleading in the full five-band model is still unclear. In any case, our analysis shows that consideration of *all* d orbitals is necessary for a proper microscopic description of multiband SC in Fe pnictides. We leave the detailed consideration of the instability of the MO incoherent metal found here to a MO SC for future consideration.

A brief discussion of the similarities and differences between cuprates and Fe pnictides is in order at this point. The predominance of normal-state incoherence in cuprates is well documented by now,⁶³ and its link with the strong on-site electronic correlations is well known. In particular, strong non-FL features [with a branch cut form of the one-particle propagator, $G(\mathbf{k}, \omega)$] in ARPES, dc and ac transport, magnetotransport, as well as in magnetic fluctuations bears this out in a very remarkable way. Up to optimal doping, the cuprates are not describable in terms of the Landau FL picture, and the role of strong Mottness and short-ranged AF spin correlations in this context is recognized. In the underdoped cuprates the instability to the d -wave SC state is quite far from the weak-coupling BCS variety: large-scale redistribution of spectral weight across T_c as well as strong vortex liquid fluctuations, short SC coherence lengths, and small superfluid stiffness, among other observations, put this transition closer to the Bose condensed limit.

Many of these features, such as normal-state incoherence, along with pseudogap behavior in *both* charge and spin fluctuations, are also characteristic of Fe pnictides. Further, in single-layer Fe pnictides, the superfluid density is small, the upper-critical fields, H_{c2} , is high, the SC in-plane coherence length is short ($\xi_{\text{pair}} < 20 \text{ \AA}$),⁵⁹ and appreciable redistribution of spectral weight across T_c is visible. These similarities then strongly support the strong correlation-based view for Fe pnictides as well.

There are noticeable differences between the cuprates and the Fe pnictides. First, SC in cuprates most likely involves a single strongly p - d hybridized band with strong electronic correlations, and arises upon doping a Mott-Hubbard insulator with AF order. In contrast, SC in Fe pnictides is most probably of the multiband variety, and arises upon doping a very bad metal, which may be close to a Mott-Hubbard insulating state.⁶ This means that the microscopic electronic glue for pairing in both cases will be quite different. Nevertheless, in view of the underlying relevance of Mottness in both cases, one may expect more similarities in the *structure*

of the SC instability in both cases. It is more likely, given the explicit MO situation in Fe pnictides, that additional competing instabilities may be at work. In particular, the nematic and current instabilities, which have been invoked as competitors of d -wave SC in cuprates,⁶⁴ might also play a role here.^{56,62} As remarked early by Baskaran,¹⁰ it is possible that being able to think about situations where these competing instabilities could be suppressed can push up the SC T_c in Fe pnictides to even higher values.

Our analysis here has been carried out for the symmetry-unbroken metallic state of the Fe pnictides. At low T , this incoherent state becomes unstable to either AF-SDW order with $\mathbf{Q}_{\text{SDW}}=\mathbf{q}=(\pi,0)$ or to SC order, depending on x , though some studies also suggest coexistence of the two orders. As discussed in literature,^{6,65} the AF-SDW state involves strong geometric frustration (GF) in the interorbital hopping matrix elements. Characterization of magnetic fluctuations has indeed been carried out, both in the strong coupling (J_1 - J_2 Heisenberg model),⁶⁶ as well as within weak-coupling HF-RPA work.⁹ Observation of features akin to high- T_c cuprates found experimentally, as discussed above, put the Fe pnictides into the strongly correlated category, though not so strongly correlated as cuprates, which are doped Mott insulators. While the fact that we are able to describe *both* the one-electron responses and the reflectivity of La pnictide strongly suggests that LDA+(MO)DMFT is adequate for a quantitative description of these correlation effects, we expect geometrical frustration effects to become relevant at low $T < T_N(x)$, at least for the SDW phase. In view of the fact that the spatial extent of correlations is short in GF systems, we remark that the dynamical effects associated with these short-ranged magnetic correlations may not change the above results substantially. They will certainly not modify them qualitatively; indeed, one would expect that additional consideration of the dynamical effects of such short-ranged strongly frustrated couplings [J_1, J_2 with J_2/J_1

$\approx O(1)$] (Ref. 65) would push the almost totally incoherent normal state derived above even more toward incoherence.

VII. CONCLUSION

In conclusion, we have studied the normal-state electrodynamic response of two Fe pnictides, $\text{La}_{1-x}\text{FeAsF}_x$ and $\text{SmO}_{1-x}\text{FeAsF}_x$, within the LDA+DMFT formalism. Armed with the very good agreement with one-electron responses (PES and XAS) between experimental and LDA+DMFT spectral functions, we *also* find very good quantitative agreement with published reflectivity data on $\text{LaO}_{1-x}\text{FeAsF}_x$. Building upon these agreements, we have studied the optical response in detail. We find an incoherent optical response, with strongly ω -dependent effective masses and transport lifetimes (scattering rates) at low energy. These features are linked to the incoherent near-pseudogaplike features found in the orbital-resolved one-particle spectral functions in LDA+DMFT. The very good agreement found between theory and experiment for *both* pnictides is strong evidence for the relevance of “Mottness,” i.e., to proximity of the normal state of Fe pnictides to a correlation-driven Mott-Hubbard insulating state. Further, based on an estimation of the “glue” function, we propose that this should be understood as arising from a multiparticle electronic continuum, which could also be interpreted in terms of an overdamped “bosonic” glue. Finally, *all* d orbitals should contribute to SC pairing, albeit anisotropically, and one should have an orbital-dependent multiple-gap SC. It is an interesting task to investigate the low- T instabilities of this incoherent metallic state: we leave this for the future.

ACKNOWLEDGMENTS

S.L. acknowledges ZIH Dresden for computational time. M.S.L. thanks the MPIPKS, Dresden for financial support.

¹Y. Kamihara, T. Watanabe, M. Hirano, and H. Hosono, *J. Am. Chem. Soc.* **130**, 3296 (2008).
²H. Luetkens, H.-H. Klauss, R. Khasanov, A. Amato, R. Klingeler, I. Hellmann, N. Leps, A. Kondrat, C. Hess, A. Köhler, G. Behr, J. Werner, and B. Büchner, *Phys. Rev. Lett.* **101**, 097009 (2008).
³K. Ahilan, F. L. Ning, T. Imai, A. S. Sefat, R. Jin, M. A. McGuire, B. C. Sales, and D. Mandrus, *Phys. Rev. B* **78**, 100501(R) (2008).
⁴D. Johrendt and R. Pöttgen, *Angew. Chem., Int. Ed.* **47**, 4782 (2008).
⁵K. Haule, J. H. Shim, and G. Kotliar, *Phys. Rev. Lett.* **100**, 226402 (2008); also, K. Haule and G. Kotliar, arXiv:0805.0722 (unpublished).
⁶Q. Si and E. Abrahams, *Phys. Rev. Lett.* **101**, 076401 (2008).
⁷A. O. Shorikov, M. A. Korotin, S. V. Streltsov, S. L. Skornyakov, D. M. Korotin, and V. I. Anisimov, arXiv:0804.3283 (unpublished).

⁸K. Kuroki, S. Onari, R. Arita, H. Usui, Y. Tanaka, H. Kontani, and H. Aoki, *Phys. Rev. Lett.* **101**, 087004 (2008).
⁹M. M. Korshunov and I. Eremin, *Phys. Rev. B* **78**, 140509(R) (2008).
¹⁰G. Baskaran, *J. Phys. Soc. Jpn.* **77**, 113713 (2008).
¹¹M. Imada, A. Fujimori, and Y. Tokura, *Rev. Mod. Phys.* **70**, 1039 (1998).
¹²J. Hubbard, *Proc. R. Soc. London, Ser. A* **276**, 238 (1963).
¹³I. I. Mazin, D. J. Singh, M. D. Johannes, and M. H. Du, *Phys. Rev. Lett.* **101**, 057003 (2008).
¹⁴S. Raghu, X. L. Qi, C. X. Liu, D. J. Scalapino, and S. C. Zhang, *Phys. Rev. B* **77**, 220503(R) (2008).
¹⁵C. de la Cruz, Q. Huang, J. W. Lynn, J. Li, W. Ratcliff II, J. L. Zarestky, H. A. Mook, G. F. Chen, J. L. Luo, N. L. Wang, and P. Dai, *Nature (London)* **453**, 899 (2008).
¹⁶J. Dong, H. J. Zhang, G. Xu, Z. Li, G. Li, W. Z. Hu, D. Wu, G. F. Chen, X. Dai, J. L. Luo, Z. Fang, and N. L. Wang, *Europhys. Lett.* **83**, 27006 (2008).
¹⁷L. Degiorgi, *Rev. Mod. Phys.* **71**, 687 (1999).

- ¹⁸M. Dressel, A. Schwartz, G. Grüner, and L. Degiorgi, *Phys. Rev. Lett.* **77**, 398 (1996).
- ¹⁹D. van der Marel, H. J. A. Molegraaf, J. Zaanen, Z. Nussinov, F. Carbone, A. Damascelli, H. Eisaki, M. Greven, P. H. Kes, and M. Li, *Nature (London)* **425**, 271 (2003).
- ²⁰S. Kimura, J. Sichelschmidt, J. Ferstl, C. Krellner, C. Geibel, and F. Steglich, *Phys. Rev. B* **74**, 132408 (2006).
- ²¹F. P. Mena, D. van der Marel, A. Damascelli, M. Fath, A. A. Menovsky, and J. A. Mydosh, *Phys. Rev. B* **67**, 241101(R) (2003).
- ²²B. S. Shastry and B. I. Shraiman, *Phys. Rev. Lett.* **65**, 1068 (1990).
- ²³H. W. Ou, J. F. Zhao, Y. Zhang, D. W. Shen, B. Zhou, L. X. Yang, C. He, F. Chen, M. Xu, T. Wu, X. H. Chen, Y. Chen, and D. L. Feng, *Chin. Phys. Lett.* **25**, 2225 (2008).
- ²⁴E. Z. Kurmaev, R. G. Wilks, A. Moewes, N. A. Skorikov, Yu. A. Izyumov, L. D. Finkelstein, R. H. Li, and X. H. Chen, *Phys. Rev. B* **78**, 220503(R) (2008).
- ²⁵L. Craco, M. S. Laad, S. Leoni, and H. Rosner, *Phys. Rev. B* **78**, 134511 (2008).
- ²⁶P. Abbamonte, A. Rusydi, S. Smadici, G. D. Gu, G. A. Sawatzky, and D. L. Feng, *Nat. Phys.* **1**, 155 (2005); P. Phillips, *Ann. Phys.* **321**, 1634 (2006).
- ²⁷A. Khurana, *Phys. Rev. Lett.* **64**, 1990 (1990).
- ²⁸S.-L. Drechsler, M. Grobosch, K. Koepfner, G. Behr, A. Koehler, J. Werner, A. Kondrat, N. Leps, Ch. Hess, R. Klingeler, R. Schuster, B. Buechner, and M. Knupfer, *Phys. Rev. Lett.* **101**, 257004 (2008).
- ²⁹S. I. Mirzaei, V. Guritanu, A. B. Kuzmenko, C. Senatore, D. van der Marel, G. Wu, R. H. Liu, and X. H. Chen, arXiv:0806.2303 (unpublished).
- ³⁰J. Yang, D. Huvonen, U. Nagel, T. Room, N. Ni, P. C. Canfield, S. L. Budko, J. P. Carbotte, and T. Timusk, arXiv:0807.1040 (unpublished).
- ³¹O. K. Andersen, *Phys. Rev. B* **12**, 3060 (1975).
- ³²The experimentally determined lattice parameters and internal positions of LaOFeAs are taken from Ref. 15. Self-consistency is reached by performing calculations on a $14 \times 14 \times 12$ **k** mesh for the Brillouin integration.
- ³³A. I. Coldea, J. D. Fletcher, A. Carrington, J. G. Analytis, A. F. Bangura, J.-H. Chu, A. S. Erickson, I. R. Fisher, N. E. Hussey, and R. D. McDonald, *Phys. Rev. Lett.* **101**, 216402 (2008).
- ³⁴K. Koepfner and H. Eschrig, *Phys. Rev. B* **59**, 1743 (1999).
- ³⁵DFT scalar relativistic calculations were performed within the LDA scheme as implemented in the all-electron full-potential local-orbital (FPLO) minimal basis method. La ($4p, 4d, 5s, 5p, 6s, 6p, 5d$), Fe ($3s, 3p, 4s, 4p, 3d$), O ($2s, 2p, 3d$), and As ($3p, 4s, 4p, 3d$) represented the basis set. Lower lying states were treated as core states. A **k** mesh of $14 \times 14 \times 10$ irreducible (1960) points in the Brillouin zone ensured convergence of the electronic part. The spatial extension of the orbitals forming the basis was optimized to minimize the total energy.
- ³⁶G. Kotliar, S. Y. Savrasov, K. Haule, V. S. Oudovenko, O. Parcollet, and C. A. Marianetti, *Rev. Mod. Phys.* **78**, 865 (2006); K. Held, *Adv. Phys.* **56**, 829 (2007).
- ³⁷M. S. Laad, L. Craco, and E. Müller-Hartmann, *Phys. Rev. Lett.* **91**, 156402 (2003); *Phys. Rev. B* **73**, 045109 (2006).
- ³⁸O. Miura and T. Fujiwara, *Phys. Rev. B* **77**, 195124 (2008).
- ³⁹F. Lechermann, S. Biermann, and A. Georges, *Phys. Rev. B* **76**, 085101 (2007).
- ⁴⁰V. I. Anisimov, Dm. M. Korotin, M. A. Korotin, A. V. Kozhevnikov, J. Kune, A. O. Shorikov, S. L. Skornyakov, and S. V. Streltsov, arXiv:0810.2629 (unpublished).
- ⁴¹J. Dai, Q. Si, J.-X. Zhu, and E. Abrahams, arXiv:0808.0305 (unpublished).
- ⁴²C. Hess, A. Kondrat, A. Narduzzo, J. E. Hamann-Borrero, R. Klingeler, J. Werner, G. Behr, and B. Büchner, arXiv:0811.1601 (unpublished).
- ⁴³T. Sato, S. Souma, K. Nakayama, K. Terashima, K. Sugawara, T. Takahashi, Y. Kamihara, M. Hirano, and H. Hosono, *J. Phys. Soc. Jpn.* **77**, 063708 (2008).
- ⁴⁴T. Kroll, S. Bonhommeau, T. Kachel, H. A. Duerr, J. Werner, G. Behr, A. Koitzsch, R. Huebel, S. Leger, R. Schoenfelder, A. Ariffin, R. Manzke, F. M. F. de Groot, J. Fink, H. Eschrig, B. Buechner, and M. Knupfer, *Phys. Rev. B* **78**, 220502 (2008).
- ⁴⁵Y. Kohama, Y. Kamihara, H. Kawaji, T. Atake, M. Hirano, and H. Hosono, *J. Phys. Soc. Jpn.* **77**, 094715 (2008).
- ⁴⁶K. Urasaki and T. Saso, *J. Phys. Soc. Jpn.* **68**, 3477 (1999); T. Saso, *ibid.* **73**, 2894 (2004).
- ⁴⁷L. Baldassarre, A. Perucchi, D. Nicoletti, A. Toschi, G. Sangiovanni, K. Held, M. Capone, M. Ortolani, L. Malavasi, M. Marsi, P. Metcalf, P. Postorino, and S. Lupi, *Phys. Rev. B* **77**, 113107 (2008).
- ⁴⁸Y. Imai and N. Kawakami, *J. Phys. Soc. Jpn.* **70**, 2365 (2001); E. Pavarini, A. Yamasaki, J. Nuss, and O. K. Andersen New, *J. Phys.* **7**, 188 (2005); L. Craco, C. I. Ventura, A. N. Yaresko, and E. Müller-Hartmann, *Phys. Rev. B* **73**, 094432 (2006).
- ⁴⁹S.-L. Drechsler (private communication).
- ⁵⁰P. Kostic, Y. Okada, N. C. Collins, Z. Schlesinger, J. W. Reiner, L. Klein, A. Kapitulnik, T. H. Geballe, and M. R. Beasley, *Phys. Rev. Lett.* **81**, 2498 (1998).
- ⁵¹D. H. Lu, M. Yi, S.-K. Mo, A. S. Erickson, J. Analytis, J.-H. Chu, D. J. Singh, Z. Hussain, T. H. Geballe, I. R. Fisher, and Z.-X. Shen, *Nature (London)* **455**, 81 (2008); T. Kondo, A. F. Santander-Syro, O. Copie, C. Liu, M. E. Tillman, E. D. Mun, J. Schmalian, S. L. Bud'ko, M. A. Tanatar, P. C. Canfield, and A. Kaminski, *Phys. Rev. Lett.* **101**, 147003 (2008).
- ⁵²S. Biermann, L. de' Medici, and A. Georges, *Phys. Rev. Lett.* **95**, 206401 (2005).
- ⁵³P. W. Anderson, *Phys. Rev. Lett.* **18**, 1049 (1967).
- ⁵⁴M. Combescot and P. Nozières, *J. Phys. (Paris)* **32**, 913 (1971), and references therein.
- ⁵⁵Q. Si and G. Kotliar, *Phys. Rev. Lett.* **70**, 3143 (1993).
- ⁵⁶A. V. Chubukov, D. V. Efremov, and I. Eremin, *Phys. Rev. B* **78**, 134512 (2008).
- ⁵⁷O. J. Lipscombe, S. M. Hayden, B. Vignolle, D. F. McMorrow, and T. G. Perring, *Phys. Rev. Lett.* **99**, 067002 (2007).
- ⁵⁸P. Richard, T. Sato, K. Nakayama, S. Souma, T. Takahashi, Y.-M. Xu, G. F. Chen, J. L. Luo, N. L. Wang, and H. Ding, arXiv:0808.1809 (unpublished).
- ⁵⁹L. Wray, D. Qian, D. Hsieh, Y. Xia, L. Li, J. G. Checkelsky, A. Pasupathy, K. K. Gomes, A. V. Fedorov, G. F. Chen, J. L. Luo, A. Yazdani, N. P. Ong, N. L. Wang, and M. Z. Hasan, *Phys. Rev. B* **78**, 184508 (2008).
- ⁶⁰A. A. Kordyuk, S. V. Borisenko, V. B. Zabolotnyy, J. Geck, M. Knupfer, J. Fink, B. Buchner, C. T. Lin, B. Keimer, H. Berger, A. V. Pan, S. Komiya, and Y. Ando, *Phys. Rev. Lett.* **97**, 017002 (2006).
- ⁶¹K. Byczuk, M. Kollar, K. Held, Y.-F. Yang, I. A. Nekrasov, Th.

- Pruschke, and D. Vollhardt, *Nat. Phys.* **3**, 168 (2007).
- ⁶²C. Fang, H. Yao, W. F. Tsai, J. P. Hu, and S. A. Kivelson, *Phys. Rev. B* **77**, 224509 (2008).
- ⁶³P. W. Anderson, *Nat. Phys.* **2**, 626 (2006).
- ⁶⁴H. Yamase and W. Metzner, *Phys. Rev. B* **75**, 155117 (2007); M. S. Grønleth, T. B. Nilssen, E. K. Dahl, C. M. Varma, and A. Sudbo, arXiv:0806.2665 (unpublished).
- ⁶⁵T. Yildirim, *Phys. Rev. Lett.* **101**, 057010 (2008).
- ⁶⁶C. Xu, M. Müller and S. Sachdev, *Phys. Rev. B* **78**, 020501(R) (2008).